Published in final edited form as:
Free Radic Biol Med. 2012 January 1; 52(1): 218–226. doi:10.1016/j.freeradbiomed.2011.10.452.

Noninvasive assessment of localized inflammatory responses

Jun Zhou[#], **Yi-Ting Tsai**[#], **Hong Weng**, and **Liping Tang**[*]
Department of Bioengineering, The University of Texas at Arlington, TX 76019

Abstract

Inflammatory diseases are associated with the accumulation of activated inflammatory cells, particularly polymorphonuclear neutrophils (PMN), which release reactive oxygen species (ROS) to eradicate foreign bodies and microorganisms. To assess the location and extent of localized inflammatory responses, L-012, a highly-sensitive chemiluminescence probe, was employed to non-invasively monitor the production of ROS. We find that L-012-associated chemiluminescence imaging can be used to identify and to quantify the extent of inflammatory responses. Furthermore, regardless of differences among animal models, there is a good linear relationship between chemiluminescence intensity and PMN numbers surrounding inflamed tissue. Depletion of PMN substantially diminished L-012-associated chemiluminescence *in vivo*. Finally, L-012-associated chemiluminescence imaging was found to be a powerful tool for assessing implant-mediated inflammatory responses by measuring chemiluminescent intensities at the implantation sites. These results support the use of L-012 for monitoring the kinetics of inflammatory responses *in vivo* via the detection and quantification of ROS production.

Keywords

Reactive oxygen species; non-invasive imaging; Inflammatory responses; Biomaterials; Chemiluminescence

Introduction

The accumulation of inflammatory phagocytes in tissue is a hallmark of all inflammatory diseases, including atherosclerosis, arthritis, dermatitis, nephritis, ulcerative colitis, psoriasis, inflammatory bowel diseases and many others [1, 2]. It is generally believed that the extent of inflammatory cell accumulation in the wound or surrounding biomaterial implants reflects the degree of inflammatory reactions. However, the numbers inflammatory cells in tissues are often hard to determine. One of the most common methods to diagnose inflammatory diseases is histological analyses of tissue biopsies involving sectioning, staining and microscopic evaluation. In addition to being invasive and un-reliable, histological analyses are time consuming, require large numbers of animals, and can only provide semi-quantitative assessment of inflammatory reactions at one time point [3–5].

[*]Correspondence to Liping Tang, Ph.D., Bioengineering Department, University of Texas at Arlington, P.O. Box 19138, Arlington, TX 76019-0138. Phone: 817-272-6075; fax: 817-272-2251; ltang@uta.edu.
[#]Both authors contributed equally to this work.

Supplementary data Experiments and results of L-012 immune response to mice can be found in the supplementary data.

Consequently, there is a need for the development of non-invasive methods to provide continuous and quantitative measurement of inflammatory responses *in vivo*.

Many cells, including macrophages/monocytes, polymorphonuclear neutrophils (PMNs), mast cells, lymphocytes, and dendritic cells, participate in the pathogenesis of inflammatory diseases [6, 7]. Among all immune cells, PMNs are the most abundant type arriving in large numbers at the injured tissue site only minutes after trauma or infection [8, 9]. Therefore, histological evaluations of PMN accumulation in the tissue are often carried out to estimate the extent of acute inflammatory responses [10, 11]. It is well documented that recruited activated PMNs activate the respiratory burst, releasing a variety of Reactive Oxygen Species (ROS), including superoxide, hydrogen peroxide, and hyperchlorous acid [12, 13]. Release of ROS may result in oxidative killing not only of foreign microorganism but also healthy cells [12, 13]. The methods used to identify and quantify these ROS include spectrophotometrical measurements, electron spin resonance spectroscopy, ELISA, and chemiluminescence [14]. These methods are well established and have been used extensively to study the extent of ROS production by PMN *in vitro*. However, most of these methods cannot be used to measure the PMN-associated ROS responses *in vivo*. Most recently, there is growing interest in the development of imaging methods to monitor ROS generation *in vivo*. Several imaging modalities have been established for ROS monitoring. These methods include electron paramagnetic resonance (EPR), fluorescence, and chemiluminescence detection [15–18]. The former two methods have been shown to have many limitations. Specifically, EPR has very low sensitivity [19]. In addition, the signal-to-noise ratio of fluorescent probes is often inadequate due to the autofluorescence generated by tissues and organs [20]. On the other hand, chemiluminescence has many advantages including high sensitivity and specificity, easy quantitative analysis, a wide dynamic range as well as localization and quantification of the light emission at the single-photon level. Furthermore, without the requirement of excitation light as in fluorescence, chemiluminescence agents can emit detectable light upon reaction with ROS generated in the biological system with minimal or no background signal [21, 22].

Recent developments in optical imaging equipment have made it possible to detect weak chemiluminescence signals in whole animals. Several chemiluminescence probes have been developed for noninvasive real time imaging *in vivo*. For example, peroxalate nanoparticles were fabricated and used as a chemiluminescence probe to detect hydrogen peroxide *in vivo* [23, 24]. Oxazine conjugated nanoparticles have been synthesized and used to detect *ex vivo* hypochlorous acid and peroxynitrite generation in mouse hearts after myocardial infarction [17]. Luminol, a chemiluminescence probe, has been used in studies to detect myeloperoxidase activity *in vivo* [25]. Finally, luminol was also used to investigate the role of ROS in the pathogenesis of arthritis and to evaluate the effectiveness of various anti-inflammatory agents as well as to detect biomaterial-induced ROS *in vivo* [26, 27]. Although these chemiluminescence probes (peroxalate nanoparticles and luminol) have shown great promise for *in vivo* monitoring of ROS activities following severe inflammatory responses, the limited sensitivity of these probes substantially hinders their use in measuring and quantifying localized inflammatory responses. Furthermore, little is known about the relationship between inflammation-mediated ROS production *in vivo* and histological measurements.

In an effort to improve these detection limits, we have applied a chemiluminescence probe, L-012 (8-amino-5-chloro-7-phenylpyridol[3,4-d]pyridazine-1,4(2H,3H) dione; a luminol derivative) which has much higher sensitivity toward ROS than other probes such as luminol and lucigenin [28, 29]. A recent study has demonstrated that L-012 is a sensitive ROS probe for *in vivo* visualization of ROS production in a model of endotoxin shock [18]. In the present study, a series of *in vitro* and *in vivo* experiments were carried out to determine the

extent of ROS production. By correlating the ROS imaging results with histological analyses, we evaluate the feasibility of using ROS chemiluminescence to non-invasively monitor the *in vivo* kinetics of localized inflammatory reactions in real time. Finally, the ROS imaging method was tested for its ability to real-time monitor foreign body responses to different types of biomaterial implants in the same animal.

Materials and methods

Materials

L-012 was purchased from Wako Chemicals. Luminol, casein, 4-hydroxy-2,2,6,6-tetramethylpiperidine 1-oxyl (tempol), phorbol 12-myristate 13-acetate (PMA), hydrogen peroxide, catalase and diethylenetriaminepentaacetic acid (DTPA) were purchased from Sigma-Aldrich. Polyurethane (PU) and heparin-bonded PU catheters were obtained from Sentry Medical Products (Green Bay, WI). Polylactic acid (PLA) microparticles (5–10 μm diameter), poly(ethylene glycol) (PEG) nanoparticles (100 nm diameter) and amine-rich poly(*N*-isopropylacrylamide-co-*N*-(3-aminopropyl) methacrylamide) (PNIPAM-NH_2) (100 nm diameter) were prepared according to the references [30–32]. PMN neutralizing antibody (Rabbit anti-Mouse PMN) was purchased from Accurate Chemical & Scientific Corporation (Westbury, NY). PMN staining antibody (rat anti-mouse neutrophil antibody) was purchased from Abcam (Cambridge, MA).

Quantification of ROS production by isolated PMNs

PMNs were isolated from mouse peritonea following casein administration as described earlier [33]. *In vitro* ROS measurements were carried out using both L-012 and luminol as chemiluminescence probes. Different numbers of PMNs (in Hanks buffered solution) were incubated with L-012 (2mM) or luminol (4mM) for 4 min at room temperature. The ROS production was then initiated by adding 10μL of PMA (6.5nM). In some experiments, tempol, a superoxide scavenger, was used to neutralize ROS products in solution. For that, cells were incubated with various concentrations of tempol prior to PMA activation. In these *in vitro* studies, chemiluminescence intensities were recorded continuously for 60 min using Luminescence Reader (Infinite M200, Tecan, Männedorf, Switzerland) with a 10 s acquisition time.

In vitro chemiluminescence imaging

In vitro imaging was carried out with black bottom 96-well plates, 200 μL of H_2O_2 solution with different concentration was mixed with 10 μL of L-012 (50 mM) [34]. The chemiluminescence images were taken 1 minute later using KODAK *In vivo* FX Pro system (Kodak, USA) (f/stop, 2.5; no optical filter, 4×4 binning).

In vivo animal model and chemiluminescence imaging

Balb/c mice (female, 20–25 gram body weight) were purchased from Taconic Farms, Inc. (Germantown, NY) and used in all *in vivo* studies. The animal protocols were approved by the Animal Studies Committee at University of Texas at Arlington. All animal tests were carried out with 6 animals per group. To detect H_2O_2-mediated chemiluminescence activities, 200 μL of H_2O_2 solution (0.5 mM) and 100 μL of L-012 (15mg/mL) were mixed at room temperature. Different volumes of solutions (20, 40, 60 and 80 μL) were injected subcutaneously on the back of anaesthetized mice (ketamine/xylazine). Chemiluminescence images were captured with a 5 min acquisition time using KODAK *In vivo* FX Pro system (f/stop, 2.5; no optical filter, 4×4 binning) and then calculated after background correction. Regions of interests (ROIs) were drawn over the implantation locations in the chemiluminescence imaging, and the mean intensities for all pixels in the

chemiluminescence imaging were calculated. All data analyses were performed with the Carestream Molecular Imaging Software, Network Edition 4.5 (Carestream Health, Woodbridge, CT).

Chemiluminescence imaging of localized inflammatory responses *in vivo*

To induce localized inflammatory responses, PLA microspheres (50 μL, 10% wt in saline) or saline as a control were implanted into different locations on the back of mice, and then a 100 μL of L-012 solution (15 mg/mL) was administered intraperitoneally at different time points. It should be noted that L-012 has very good biocompatibility and low toxicity [18]. Our preliminary experiments showed that L-012 has no apparent effect on immune responses of animals up to 150mg/kg (supplementary Fig. 1). The non- or low toxicity nature of L-012 permits their use in cell culture study and animal work. Chemiluminescence images were captured sequentially every 5 min up to 1 hour. Similar experiments were carried out using PMN-depleted mice which were produced based on a modified published protocol [35]. In brief, 100 μL of PMN neutralizing antibody (Rabbit anti-Mouse PMN, Accurate Chemical & Scientific Corporation, Westbury, NY) was injected intraperitoneally (ip) and 18 hours later a second injection of 100 μL antibody was given ip. Four hours after the second injection, 50 μL of PLA particles (10% w/v) were implanted subcutaneously on the back of the PMN-depleted mouse and a control mouse. The chemiluminescence imaging was taken 24 hours after PLA implantation. To investigate effects of either catalase (a scavenger of hydrogen peroxide) or DTPA (a metal chelator) on implant-mediated chemiluminescence [36–38], 50 μL of PLA particles (10% wt) were mixed with either catalase (500 units/mL), DTPA (1mM), or saline (as control) prior to subcutaneous implantation followed by chemiluminescence imaging after 24 hour implantation as described above.

Inflammatory animal models

To trigger different extents of inflammatory responses in the same animals, PNIPAM-NH_2, PLA, PEG particles (50 μL, 10% w/v) and saline (control) were injected subcutaneously into different locations on the back of mice, respectively. To mimic infection-mediated inflammatory responses, 100μg/50 μl of LPS were administered subcutaneously on the back of Balb/C mice while the treatment of saline alone was used as controls. To elicit skin allergenic responses, some animals were subcutaneously injected with 100μg of c48/80 or saline. To monitor different extent of foreign body reactions, PU catheter and Heparinized PU (H-PU) catheters (1 cm length) from Sentry Medical Products (city, IL)) was implanted subcutaneously on the back of mice. The extent of the chemiluminescence signal was detected and quantified at 24 hours following the treatment of inflammatory stimuli.

Histochemical analysis and inflammatory cell quantification

At the end of the study, the test animals were sacrificed and the implantation sites/inflamed tissues were isolated for histological analyses. All tissues sections were subjected to H&E or immunohistochemical staining for PMNs based on established protocols [3, 39].

Statistical analysis

Statistical comparison between different treatment groups was carried out using student's t test. Differences were considered statistically significant when $p \leq 0.05$. Linear regression analyses were also used to determine the correlation coefficient between PMN densities and chemiluminescence signal intensities.

Results

To search for a sensitive chemiluminescence probe, we compared the ROS detection sensitivity of L-012 vs. luminol. Mice peritoneal PMNs were incubated with L-012 in the presence of potent protein kinase C activator - phorbol 12-myristate-13-acetate (PMA). We found that with PMA activation, both luminol and L-012 emitted chemiluminescence in a time-dependent manner. Chemiluminescence of L-012 (Figure 1a) initially increases with time and peaks at ~30 minutes after stimulation while the maximal chemiluminescence of luminol appears at ~15 minutes. Based on the peak value of the two probes, we observed that the signal intensity generated by the L-012 is approximately 900 fold greater than that generated by luminol (Figure 1b). To further determine its ROS sensitivity, L-012 was exposed to increasing numbers of PMNs. As expected, ROS prompt strong emission of chemiluminescence and chemiluminescence intensities are cell number dependent (Figure 1c). In addition, there was a linear relationship between the chemiluminescence intensity and activated PMN numbers ($R^2 = 0.95$) (Figure 1d). To verify whether chemiluminescence signals resulted from ROS generated by activated PMNs, similar PMN-mediated chemiluminescence measurements were carried out in the presence or absence of a superoxide dismutase mimetic/ROS neutralizer–tempol (4-hydroxy-2,2,6,6-tetramethylpiperidine-N-oxyl). As anticipated, the chemiluminescence intensity was substantially reduced in the presence of as low as 5 mM of tempol (Figure 1e). Collectively, these data indicate that L-012 can be used to estimate the numbers of activated PMN based on their ROS-mediated chemiluminescence signals. These results support that L-012 chemiluminescence probes may be used to quantify the extent of PMN-associated ROS production.

Subsequent studies were carried out to evaluate the feasibility of L-012 for *in vivo* whole body imaging. First, L-012 was used to detect hydrogen peroxide *in vitro* with a Kodak *in vivo* FX imaging system. As expected, chemiluminescence intensity of L-012 increased with the increase of hydrogen peroxide concentrations from 0.05 to 0.5 mM (Figure 2a), and there was a linear correlation between chemiluminescence intensities and the concentrations of hydrogen peroxide (Figure 2a). Second, to determine whether L-012-mediated chemiluminescence signals might be used to measure ROS release *in vivo*, various volumes (20, 40, 60, 80 μL) of H_2O_2 (0.5mM) mixed with L-012 (15mg/mL) were injected subcutaneously in diseased animals and then imaged. As anticipated, L-012 could detect subcutaneous H_2O_2, which was also found to have a linear correlation between H_2O_2 quantities and chemiluminescence intensities (Figure 2b).

Finally, to assess whether L-012-mediated chemiluminescence can be used to assess ROS production arising *in vivo* from a known pro-inflammatory agent, poly-lactic acid (PLA) microspheres (50μl in 10% wt) or saline, as a control, were administered subcutaneously on the back of live mice. Implants were followed by intraperitoneal administration of a 15 mg/mL L-012 solution at different time points. Our results show that a prominent chemiluminescence signal could be detected at the PLA implant site while only minimal signal was detected at the saline injected site (Figure 3a & b). Interestingly, histological analyses also revealed that there are substantially more PMNs in tissue surrounding 1-day implants than those nearby 7-day implants (Figure 3c & the inset of Figure 3d). In addition, there was a good linear relationship between chemiluminescence intensities (ROS activities) and the infiltrated PMNs (R^2=0.94, Figure 3d). These results reveal that L-012 can be used to non-invasively monitor real time inflammation-induced ROS generation *in vivo*.

Since it has been well established that PMNs are one of the most potent cells in producing ROS, we assumed that PMN-mediated ROS would be responsible for L-012-dependent chemiluminescence signals. To test this, similar studies were carried out in neutropenic

mice. Pre-treatment of mice with anti-PMN antibodies reduced chemiluminescence by approximately 70% at the PLA implantation site compared to control mice (Figure 4a & b). Interestingly, histological evaluation also revealed a ~60% reduction in infiltrating PMNs at the implantation site in PMN-depleted mice compared to control mice (Figure 4c & d). Correlation analysis suggests a linear relationship between chemiluminescence intensities and numbers of recruited PMNs (Figure 4e), supporting the idea that PMN-generated ROS are primarily responsible for L-012-depedent chemiluminescence signals. To determine the type of ROS detected with the L-012 probe, catalase, a potent enzyme for neutralizing H_2O_2, was injected into the implant sites prior to L-012 administration. Indeed, the treatment of catalase substantially reduced (~65%) the chemiluminescent intensities (Fig. 4f). Further studies were conducted to investigate whether metal ions participate in ROS responses, using an iron chelator – DTPA. As expected, the presence of DTPA had no significant impact on chemiluminescent intensity compared to control suggesting that H_2O_2 is a major type of ROS product generated as part of foreign body reactions (Figure 4f).

Despite the above results, it remained unclear whether other pro-inflammatory stimuli might have similar effects on L-012-mediated chemiluminescence. To test this, three different types of inflammatory models – LPS-mediated inflammation, histamine-induced inflammation and medical device-associated tissue responses - were used. First, an LPS-mediated inflammation model was established as previously described [40]. Briefly, LPS and saline, as a control, were injected subcutaneously, and then 100 μL of L-012 (15mg/mL) was administrated intraperitoneally 24 hours after LPS/saline injection. It is well known that LPS administration can elicit a acute inflammation and therefore increase ROS and Reactive Nitrogen Species (RNS) production by immune cells [41, 42]. Indeed, substantial L-012-mediated chemiluminescence signals were found at the site of LPS injection (Figure 5a). The site with LPS treatment had a chemiluminescence intensity of 5.8×10^8 photons/s while the control site with saline injection had an intensity of 8.8×10^6 photons/s.

In a different model, dermal inflammation was induced by injection of c48/80 which causes histamine release from mast cells [43, 44] and the subsequent recruitment of PMNs [45–47]. A substantial increase of the chemiluminescence signal (8 times) was found in the region of c48/80 administration compared to controls (areas with saline injection) (Figure 5b). To mimic foreign body reactions to medical devices, polyurethane (PU) catheters and heparinized PU catheters (H-PU) were implanted on the backs of Balb/C mice. Twenty-four hours after implantation, we measured L-012-mediated chemiluminescence. As expected, a relatively (3×) strong signal was emitted from the PU implantation site compared to that from the H-PU catheter site, whereas sites at which similar wounds (without implant placement) exhibited very weak chemiluminescence (Figure 5c). Histological analysis for all three inflammatory models tested indicated that there was a good linear relationship between inflammatory responses (i.e., PMN recruitment) and L012-dependent chemiluminescence signals (R^2=0.87, Figure 5d).

Subsequent studies were designed to test whether L-012-mediated ROS measurements might be used to assess the extent of inflammatory responses to materials known to have varying pro-inflammatory effects *in vivo*. Biomaterial implants trigger an array of foreign body reactions and PMNs play an important role in biomaterial-mediated acute inflammatory responses [48–50]. Three different types of polymeric particles made of poly-lactic acid (PLA), polyethylene glycol (PEG), and amine-rich poly(*N*-isopropylacrylamide-co-*N*-(3-aminopropyl) methacrylamide) (PNIPAM-NH_2) were used. A 50μl solution of various implants (10% w/v) and saline as a control were injected subcutaneously in the dorsal region of mice. One day after implantation, L-012-dependent chemiluminescence intensities at different implant sites were determined and chemiluminescence varied in the following order: PNIPAM-NH_2 > PLA > PEG > saline control (Figure 6a & b). Specifically,

chemiluminescence intensities generated from PNIPAM-NH_2, PLA and PEG implant site were ~52, 16 and 4 times higher than that caused by saline injection alone. Histological evaluations also revealed that the trend of phagocytes (H&E staining) and PMN (immunohistochemical staining) recruitment is similar to that of chemiluminescence intensities (Figure 6c-d). The densities of PMNs in tissue surrounding PNIPAM-NH_2 implants were 3 and 6 times higher than those surrounding PLA and PEG particle implants, respectively. There was a linear relationship between PMN numbers and L-012 chemiluminescence intensities (Figure 6e). These results verify that L-012 chemiluminescence signal monitoring may be used to determine the extent of inflammatory responses to various inflammatory mediators in the same animals.

Discussion

Many ROS probes, including luminophores, chromogenic probes and fluorescent probes, have been developed to detect ROS activities *in vitro* and *in vivo*. In agreement with several recent findings, our results show that L-012 is a highly-sensitive ROS probe with a superior signal to noise ratio [28, 29]. and is a reliable probe for non-invasive detection of ROS responses *in vivo* [18]. By comparison with luminol, a commonly-used chemiluminescence probe [25, 26]. we found that L-012 emits a considerably stronger signal (~900 times higher), in agreement with a previous *in vitro* study [51]. The comparatively low chemiluminescence emission of luminol may be partially caused by the fact that the luminol signal is pH dependent showing a reduction at low pH, which often occurs at sites of inflammation [52]. Further, the results of H_2O_2 concentration-dependent chemiluminescence for L-012 show good agreement with a previous study in which ROS-mediated L-012 chemiluminescence are generated by xanthine oxidase [51].

L-012-dependent chemiluminescence signals have been used in an earlier study to detect inflammation-mediated ROS release *in vivo* [18]. However, it was not clear whether L-012-associated chemiluminescence signals can be used to monitor, and especially to quantify, the extent of inflammatory responses. Our *in vitro* cell culture and *in vivo* cell depletion studies have confirmed that activated PMNs are mainly responsible for L-012-dependent chemiluminescence signals. These findings are in agreement with many previous observations. First, the accumulation of PMNs in the tissues is the hallmark of inflammatory responses [8–11]. Second, as part of the immune defense system's response to inflammation, recruited PMNs release a variety of ROS in response to inflammatory stimuli, including bacteria, infection, trauma, and implant-mediated inflammation [13, 53]. Finally, PMN-derived myeloperoxidase is responsible for ROS production, since myeloperoxidase-knockout mice were found to cause reduced luminol-dependent chemiluminescence signals [25]. Furthermore, a 65% reduction of L-012-mediated chemiluminescence in the presence of catalase indicates that L-012 is able to react with other ROS products besides H_2O_2. This finding is supported by previous observations that L-012 can respond to superoxide, peroxynitrite or nitric oxide to emit chemiluminescence [18, 28, 51].

Our results show that L-012-dependent chemiluminescence signals can be used to detect and to assess the extent and kinetics of inflammatory reactions over time. Such real-time measurements cannot be achieved using conventional methods, including histological analyses and inflammatory marker measurements [54, 55]. Our results with biomaterial implants indicate that the strongest chemiluminescence signal appears at day 1 in agreement with earlier reports that PMN accumulation peaks 1–2 days after biomaterial implantation [3]. In addition, real time measurements allow us to assess the kinetics of inflammatory responses with a minimal number of animals. For example, while several groups of animals are needed for histological analyses for different time points, the use of L-012-dependent

chemiluminescence measurement permits the measurement of inflammatory responses for all time points with one group of animals.

This study also explored the possibility of using L012-associated ROS measurements to quantify various other types of inflammatory responses. For that, infection- and allergy-mediated inflammatory responses were induced by subcutaneous injection of LPS (bacterial toxin) and c48/80 (mast cell activator) [18, 40, 45, 46]. We find significant increases of L-012-depedent chemiluminescence intensities in the injection sites of both types of inflammatory stimuli. These findings are supported by previous observations that PMNs quickly produce and secrete ROS after exposure to bacterial endotoxin LPS or c48/80 [42, 56]. In another model, we assessed ROS activities surrounding various intravenous catheters. Polyurethane (PU) catheters have been widely used in biomedical practice for drug administration, parenteral nutrition, fluid replacement and IV bags due to their excellent mechanical properties and low cell toxicity [57]. To improve their blood compatibility, heparinized PU catheters have been produced which have also been shown to trigger substantially less inflammatory responses than uncoated catheters [58, 59]. Indeed, our results show that heparinized PU catheters prompt reduced ROS activities compared to uncoated catheters. Furthermore, rather importantly, we find that there is a good relationship between chemiluminescence signals and different types of inflammatory responses *in vivo*. Overall, these results support the conclusion that L-012-associated ROS measurements can be used to continuously monitor the kinetics of inflammatory reactions in various inflammatory disease models.

Finally, it is well documented that biomaterial implants prompt varying inflammatory responses [50]. By testing three different types of polymeric particles (PLA, PNIPAM-NH_2 and PEG) with different biocompatibilities [60, 61], our studies show that there is a very good linear relationship between chemiluminescence intensities and histological inflammatory measurements. As expected, the stronger inflammatory reactions are accompanied with higher L-012-dependent chemiluminescence intensities. These results demonstrate that measurements of *in vivo* generation of ROS using L-012 can be utilized as a powerful tool to simultaneously assess the extent of inflammatory responses to different implants in an animal, which eliminates the variations in immune reactions between animals. These quantitative measurements may not be possible using less sensitive ROS probes, such as luminal [27].

In conclusion, our studies have established that L-012-mediated chemiluminescence imaging can serve as a promising tool for *in vivo* examining of ROS activities of activated PMNs during inflammatory processes in living animals. The advantages of this method over traditional techniques include simplicity, low cost, continuous measurements, and reduced animal numbers. Finally, this novel technique could provide in-depth and quantitatively perceptive insights on different treatments for altering immune reactions *in vivo*.

Supplementary Material

Refer to Web version on PubMed Central for supplementary material.

Acknowledgments

This work was supported by NIH grant EB007271. The authors acknowledge Professor John W. Eaton for his critical review of this work.

Abbreviations

PMNs	polymorphonuclear neutrophils
ROS	reactive oxygen species
RNS	reactive nitrogen species
L-012	8-amino-5-chloro-7-phenylpyrido[3,4-d]pyridazine-1,4(2H,3H)dione
EPR	electron paramagnetic resonance
Tempol	4-hydroxy-2,2,6,6-tetramethylpiperidine 1-oxyl
PMA	phorbol 12-myristate 13-acetate
c48/80	compound 48/80
LPS	lipopolysaccharide
DTPA	diethylenetriaminepentaacetic acid
PU	polyurethane
H-PU	heparin-bonded polyurethane
PLA	polylactic acid
PEG	poly(ethylene glycol)
PNIPAM-NH_2	poly(N-isopropylacrylamide-co-N-(3-aminopropyl)methacrylamide)
ROIs	regions of interests
H&E	hematoxylin-eosin stain

References

1. Dannenberg AM Jr. Macrophages in inflammation and infection. N Engl J Med. 1975; 293:489–93. [PubMed: 1097912]
2. Savill JS, Wyllie AH, Henson JE, Walport MJ, Henson PM, Haslett C. Macrophage phagocytosis of aging neutrophils in inflammation. Programmed cell death in the neutrophil leads to its recognition by macrophages. J Clin Invest. 1989; 83:865–75. [PubMed: 2921324]
3. Baker DW, Liu X, Weng H, Luo C, Tang L. Fibroblast/fibrocyte: surface interaction dictates tissue reactions to micropillar implants. Biomacromolecules. 2011; 12:997–1005. [PubMed: 21332193]
4. Sabaliauskas NA, Foutz CA, Mest JR, Budgeon LR, Sidor AT, Gershenson JA, et al. High-throughput zebrafish histology. Methods. 2006; 39:246–54. [PubMed: 16870470]
5. Gerstner AO, Trumpfheller C, Racz P, Osmancik P, Tenner-Racz K, Tarnok A. Quantitative histology by multicolor slide-based cytometry. Cytometry A. 2004; 59:210–9. [PubMed: 15170600]
6. Anderson JM. Biological responses to materials. Annu Rev Mater Res. 2001; 31:81–110.
7. Luttikhuizen DT, Harmsen MC, Van Luyn MJA. Cellular and molecular dynamics in the foreign body reaction. Tissue Eng. 2006; 12:1955–70. [PubMed: 16889525]
8. Yurt RW, Pruitt BA Jr. Decreased wound neutrophils and indiscrete margination in the pathogenesis of wound infection. Surgery. 1985; 98:191–8. [PubMed: 4023919]
9. Martin P, Leibovich SJ. Inflammatory cells during wound repair: the good, the bad and the ugly. Trends Cell Biol. 2005; 15:599–607. [PubMed: 16202600]
10. Romson JL, Hook BG, Kunkel SL, Abrams GD, Schork MA, Lucchesi BR. Reduction of the extent of ischemic myocardial injury by neutrophil depletion in the dog. Circulation. 1983; 67:1016–23. [PubMed: 6831665]
11. Neumann FJ, Ott I, Gawaz M, Richardt G, Holzapfel H, Jochum M, et al. Cardiac release of cytokines and inflammatory responses in acute myocardial infarction. Circulation. 1995; 92:748–55. [PubMed: 7543831]

12. Greenhalgh DG. The role of apoptosis in wound healing. Int J Biochem Cell Biol. 1998; 30:1019–30. [PubMed: 9785465]
13. Cazenave, JP.; Davies, JA.; Kazatchkine, MD.; Van Aken, WG., editors. Blood-surface interactions: biological principles underlying haemocompatibility with artificial materials. Amsterdam: Elsevier; 1986.
14. Halliwell B, Whiteman M. Measuring reactive species and oxidative damage in vivo and in cell culture: how should you do it and what do the results mean? Brit J Pharmacol. 2004; 142:231–55. [PubMed: 15155533]
15. Hirayama A, Nagase S, Ueda A, Oteki T, Takada K, Obara M, et al. In vivo imaging of oxidative stress in ischemia-reperfusion renal injury using electron paramagnetic resonance. Am J Physiol-Renal. 2005; 288:F597–F603.
16. Burks SR, Ni JH, Muralidharan S, Coop A, Kao JPY, Rosen GM. Optimization of Labile Esters for Esterase-Assisted Accumulation of Nitroxides into Cells: A Model for In Vivo EPR Imaging. Bioconjugate Chem. 2008; 19:2068–71.
17. Panizzi P, Nahrendorf M, Wildgruber M, Waterman P, Figueiredo JL, Aikawa E, et al. Oxazine Conjugated Nanoparticle Detects in Vivo Hypochlorous Acid and Peroxynitrite Generation. J Am Chem Soc. 2009; 131:15739–44. [PubMed: 19817443]
18. Kielland A, Blom T, Nandakumar KS, Holmdahl R, Blomhoff R, Carlsen H. In vivo imaging of reactive oxygen and nitrogen species in inflammation using the luminescent probe L-012. Free Radical Bio Med. 2009; 47:760–6. [PubMed: 19539751]
19. Shulaev V, Oliver DJ. Metabolic and proteomic markers for oxidative stress. New tools for reactive oxygen species research. Plant Physiol. 2006; 141:367–72. [PubMed: 16760489]
20. Frangioni JV. In vivo near-infrared fluorescence imaging. Curr Opin Chem Biol. 2003; 7:626–34. [PubMed: 14580568]
21. le Masne de Chermont Q, Chaneac C, Seguin J, Pelle F, Maitrejean S, Jolivet JP, et al. Nanoprobes with near-infrared persistent luminescence for in vivo imaging. Proc Natl Acad Sci U S A. 2007; 104:9266–71. [PubMed: 17517614]
22. Roda A, Guardigli M, Pasini P, Mirasoli M, Michelini E, Musiani M. Bio- and chemiluminescence imaging in analytical chemistry. Anal Chim Acta. 2005; 541:25–36.
23. Lee D, Khaja S, Velasquez-Castano JC, Dasari M, Sun C, Petros J, et al. In vivo imaging of hydrogen peroxide with chemiluminescent nanoparticles. Nat Mater. 2007; 6:765–9. [PubMed: 17704780]
24. Lee D, Erigala VR, Dasari M, Yu J, Dickson RM, Murthy N. Detection of hydrogen peroxide with chemiluminescent micelles. Int J Nanomedicine. 2008; 3:471–6. [PubMed: 19337415]
25. Gross S, Gammon ST, Moss BL, Rauch D, Harding J, Heinecke JW, et al. Bioluminescence imaging of myeloperoxidase activity in vivo. Nat Med. 2009; 15:455–61. [PubMed: 19305414]
26. Chen WT, Tung CH, Weissleder R. Imaging reactive oxygen species in arthritis. Mol Imaging. 2004; 3:159–62. [PubMed: 15530251]
27. Liu WF, Ma M, Bratlie KM, Dang TT, Langer R, Anderson DG. Real-time in vivo detection of biomaterial-induced reactive oxygen species. Biomaterials. 2010; 32:1796–1801. [PubMed: 21146868]
28. Daiber A, August M, Baldus S, Wendt M, Oelze M, Sydow K, et al. Measurement of NAD(P)H oxidase-derived superoxide with the luminol analogue L-012. Free Radic Biol Med. 2004; 36:101–11. [PubMed: 14732294]
29. Daiber A, Oelze M, August M, Wendt M, Sydow K, Wieboldt H, et al. Detection of superoxide and peroxynitrite in model systems and mitochondria by the luminol analogue L-012. Free Radic Res. 2004; 38:259–69. [PubMed: 15129734]
30. Zhou T, Wu WT, Zhou SQ. Engineering oligo(ethylene glycol)-based thermosensitive microgels for drug delivery applications. Polymer. 2010; 51:3926–33.
31. Zhou J, Cai T, Tang S, Marquez M, Hu Z. Growth of columnar hydrogel colloidal crystals in water-organic solvent mixture. Langmuir. 2006; 22:863–6. [PubMed: 16430238]
32. Jain RA. The manufacturing techniques of various drug loaded biodegradable poly(lactide-co-glycolide) (PLGA) devices. Biomaterials. 2000; 21:2475–90. [PubMed: 11055295]

33. Luo Y, Dorf ME. Isolation of mouse neutrophils. Curr Protoc Immunol. 2001; 20:1–6. [PubMed: 18432774]
34. Floyd RA. Observations on Nitroxyl Free-Radicals in Arylamine Carcinogenesis and on Spin-Trapping Hydroxyl Free-Radicals. Can J Chem. 1982; 60:1577–86.
35. Hao Q, Chen Y, Zhu Y, Fan Y, Palmer D, Su H, et al. Neutrophil depletion decreases VEGF-induced focal angiogenesis in the mature mouse brain. J Cereb Blood Flow Metab. 2007; 27:1853–60. [PubMed: 17392691]
36. Zorov DB, Filburn CR, Klotz LO, Zweier JL, Sollott SJ. Reactive oxygen species (ROS)-induced ROS release: a new phenomenon accompanying induction of the mitochondrial permeability transition in cardiac myocytes. J Exp Med. 2000; 192:1001–14. [PubMed: 11015441]
37. Zulueta JJ, Sawhney R, Yu FS, Cote CC, Hassoun PM. Intracellular generation of reactive oxygen species in endothelial cells exposed to anoxia-reoxygenation. Am J Physiol. 1997; 272:L897–902. [PubMed: 9176254]
38. Kumar A, Mishra P, Ghosh S, Sharma P, Ali M, Pandey BN, et al. Thorium-induced oxidative stress mediated toxicity in mice and its abrogation by diethylenetriamine pentaacetate. Int J Radiat Biol. 2008; 84:337–49. [PubMed: 18386198]
39. Kamath S, Bhattacharyya D, Padukudru C, Timmons RB, Tang L. Surface chemistry influences implant-mediated host tissue responses. J Biomed Mater Res A. 2008; 86:617–26. [PubMed: 18022841]
40. Zhou J, Tsai Y, Weng H, Baker DW, Tang L. Real time monitoring of biomaterial-mediated inflammatory responses via macrophage-targeting NIR nanoprobes. Biomaterials. 2011; 32:9383–9390. [PubMed: 21893338]
41. Park HS, Jung HY, Park EY, Kim J, Lee WJ, Bae YS. Cutting edge: direct interaction of TLR4 with NAD(P)H oxidase 4 isozyme is essential for lipopolysaccharideinduced production of reactive oxygen species and activation of NF-kappa B. J Immunol. 2004; 173:3589–93. [PubMed: 15356101]
42. Miletic AV, Graham DB, Montgrain V, Fujikawa K, Kloeppel T, Brim K, et al. Vav proteins control MyD88-dependent oxidative burst. Blood. 2007; 109:3360–8. [PubMed: 17158234]
43. Sun YG, Zhao ZQ, Meng XL, Yin J, Liu XY, Chen ZF. Cellular basis of itch sensation. Science. 2009; 325:1531–4. [PubMed: 19661382]
44. Liu T, Xu ZZ, Park CK, Berta T, Ji RR. Toll-like receptor 7 mediates pruritus. Nat Neurosci. 2010; 13:1460–2. [PubMed: 21037581]
45. Tomoe S, Iwamoto I, Tomioka H, Yoshida S. Comparison of substance P-induced and compound 48/80-induced neutrophil infiltrations in mouse skin. Int Arch Allergy Immunol. 1992; 97:237–42. [PubMed: 1375205]
46. Riley JF, West GB. Tissue mast cells: studies with a histamine-liberator of low toxicity (compound 48/80). J Pathol Bacteriol. 1955; 69:269–82. [PubMed: 13243195]
47. McGowen AL, Hale LP, Shelburne CP, Abraham SN, Staats HF. The mast cell activator compound 48/80 is safe and effective when used as an adjuvant for intradermal immunization with Bacillus anthracis protective antigen. Vaccine. 2009; 27:3544–52. [PubMed: 19464533]
48. Zdolsek J, Eaton JW, Tang L. Histamine release and fibrinogen adsorption mediate acute inflammatory responses to biomaterial implants in humans. J Transl Med. 2007; 5:31. [PubMed: 17603911]
49. Hu WJ, Eaton JW, Ugarova TP, Tang L. Molecular basis of biomaterial-mediated foreign body reactions. Blood. 2001; 98:1231–8. [PubMed: 11493475]
50. Tang L, Hu W. Molecular determinants of biocompatibility. Expert Rev Med Devices. 2005; 2:493–500. [PubMed: 16293087]
51. Imada I, Sato EF, Miyamoto M, Ichimori Y, Minamiyama Y, Konaka R, et al. Analysis of reactive oxygen species generated by neutrophils using a chemiluminescence probe L-012. Anal Biochem. 1999; 271:53–8. [PubMed: 10361004]
52. Samuni A, Krishna CM, Cook J, Black CD, Russo A. On radical production by PMA-stimulated neutrophils as monitored by luminol-amplified chemiluminescence. Free Radic Biol Med. 1991; 10:305–13. [PubMed: 1649785]

53. Valko M, Leibfritz D, Moncol J, Cronin MT, Mazur M, Telser J. Free radicals and antioxidants in normal physiological functions and human disease. Int J Biochem Cell Biol. 2007; 39:44–84. [PubMed: 16978905]
54. Lademann J, Otberg N, Richter H, Meyer L, Audring H, Teichmann A, et al. Application of optical non-invasive methods in skin physiology: a comparison of laser scanning microscopy and optical coherent tomography with histological analysis. Skin Res Technol. 2007; 13:119–32. [PubMed: 17374052]
55. Mason, WT. Fluorescent and luminescent probes for biological activity: a practical guide to technology for quantitative real-time analysis. 2. San Diego: Academic Press; 1999.
56. Yang Z, Marshall JS. Zymosan treatment of mouse mast cells enhances dectin-1 expression and induces dectin-1-dependent reactive oxygen species (ROS) generation. Immunobiology. 2009; 214:321–30. [PubMed: 19327548]
57. Krafte-Jacobs B, Sivit CJ, Mejia R, Pollack MM. Catheter-related thrombosis in critically ill children: comparison of catheters with and without heparin bonding. J Pediatr. 1995; 126:50–4. [PubMed: 7815223]
58. Heyman PW, Cho CS, McRea JC, Olsen DB, Kim SW. Heparinized polyurethanes: *In vitro* and *in vivo* studies. Journal of Biomedical Materials Research. 1985; 19:419–436. [PubMed: 4055825]
59. Krafte-Jacobs B, Sivit CJ, Mejia R, Pollack MM. Catheter-related thrombosis in critically ill children: comparison of catheters with and without heparin bonding. J Pediatr. 1995; 126:50–4. [PubMed: 7815223]
60. Hoffmann J, Groll J, Heuts J, Rong HT, Klee D, Ziemer G, et al. Blood cell and plasma protein repellent properties of Star-PEG-modified surfaces. J Biomat Sci-Polym E. 2006; 17:985–96.
61. Weng H, Zhou J, Tang LP, Hu ZB. Tissue responses to thermally-responsive hydrogel nanoparticles. J Biomat Sci-Polym E. 2004; 15:1167–80.

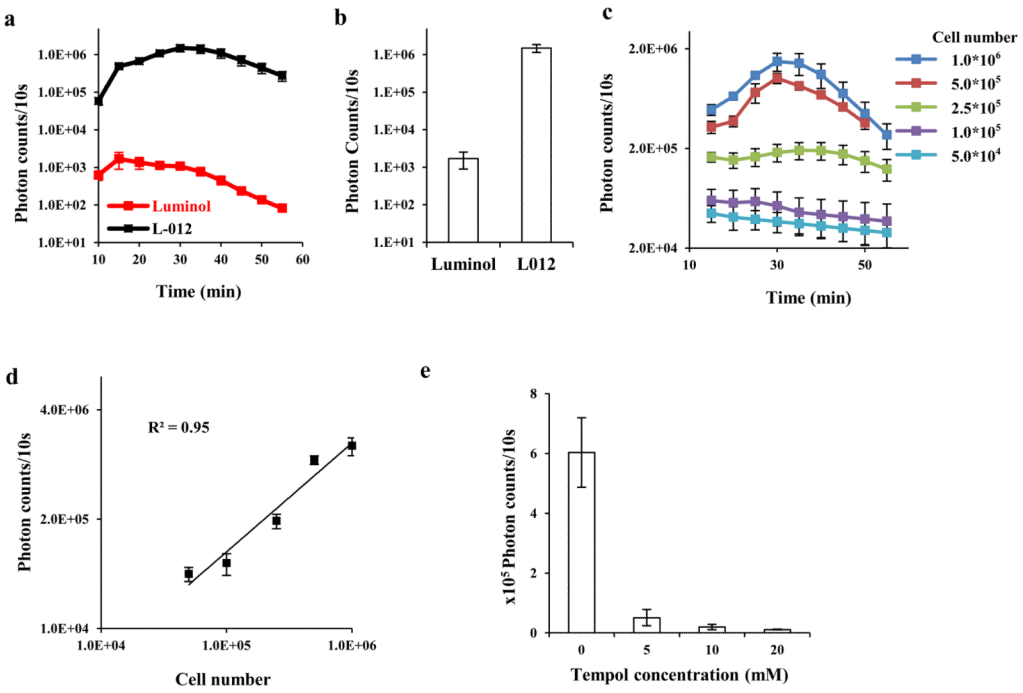

Figure 1.

(a) Time-dependent chemiluminescence intensity for L-012 and luminol. Reaction mixtures (250 μL) contained 1×10^6 PMNs, and 2 mM L-012 or 4mM luminol. The ROS measurements were initiated by adding 10μL of PMA (6.5nM) at room temperature; (b) The average chemiluminescence intensity obtained at the peak points for L-012 and luminol; (c) Dynamic L-012 chemiluminescence of PMA-stimulated PMNs with different cell numbers. Chemiluminescence was monitored for 60 min; (d) Linear curve between chemiluminescence intensities and PMN numbers was derived from the 30-min time point; (e) Supplement of tempol inhibits L-012 chemiluminescence emitted by PMA-stimulated PMNs (1×10^6).

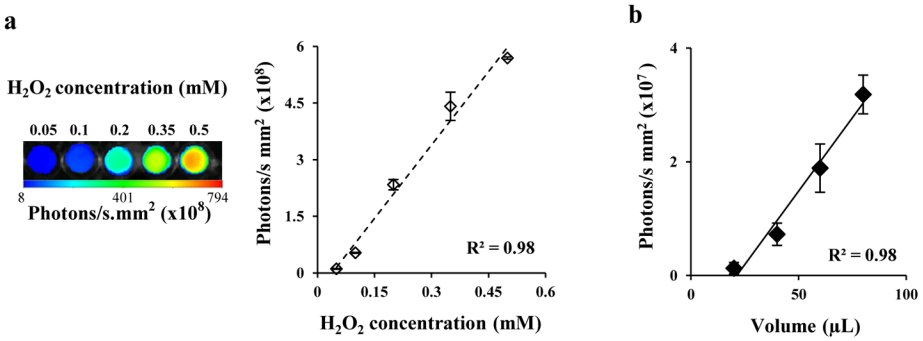

Figure 2.

(a) *In vitro* imaging and quantification of L-012-mediated chemiluminescence at various concentrations of H_2O_2. (b) Correlations between H_2O_2 dosage and *in vivo* L-012-mediated chemiluminescence.

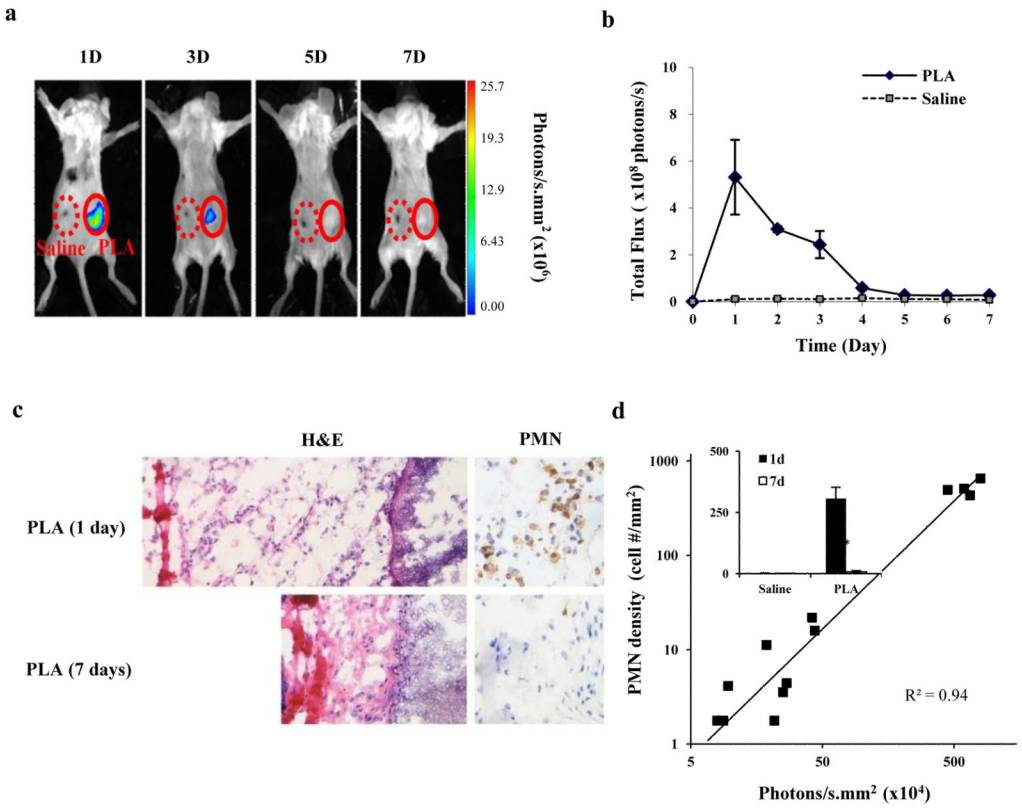

Figure 3.

(a) *In vivo* chemiluminescence imaging of animal subcutaneously implanted with PLA microspheres and saline (as control) for different periods of time; (b) L-012 chemiluminescence intensities at the implant sites at different time points; (c) H&E and anti-PMN IHC staining on implant-surrounding tissues isolated at day one or day seven; (f) Correlations between PMN numbers and chemiluminescence intensities in implant-associated tissue at different time points (The figure inset represents PMN number counts for PLA implants and controls at day 1 and day 7).

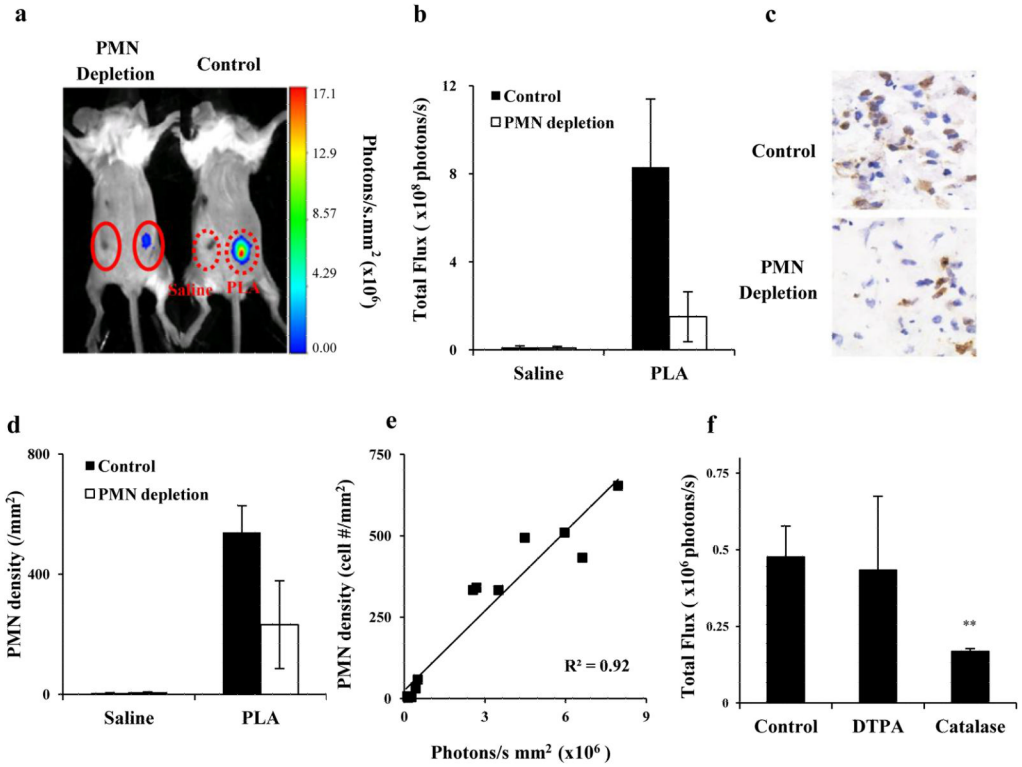

Figure 4.

(a) Chemiluminescence imaging of PLA-mediated inflammatory responses in control and PMN-depleted mice taken one day after implantation; (b) Chemiluminescence intensities at the implant sites; (c) Histological staining of tissues in the implantation sites isolated from both groups of animals; (d) Measurement of mean densities of tissue PMNs (per square millimeter); (e) Correlation between PMN numbers and chemiluminescence intensities in tissue isolated from variously treated animals; (f) Effect of either catalase or DTPA on chemiluminescent signal of PLA-mediated inflammatory responses.

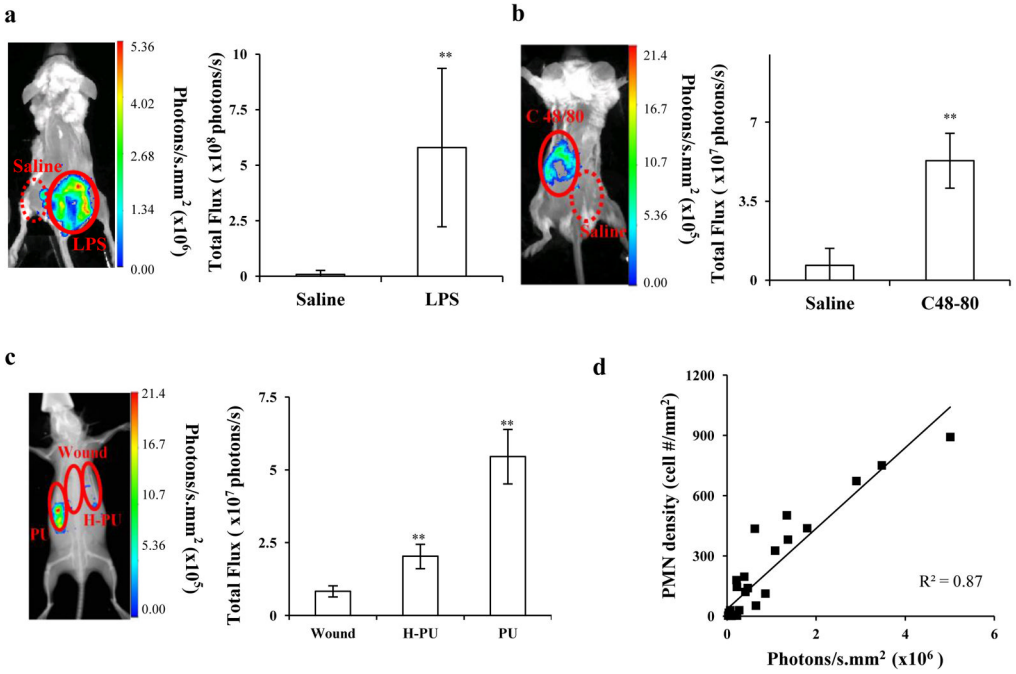

Figure 5.

(a) L-012-mediated chemiluminescence imaging and intensities in mice with LPS-induced inflammatory responses, (b) with skin allergic response induced by subcutaneous injection of c48/80; or (c) implanted subcutaneously with heparinized PU and PU catheters which prompted different extent of immune reactions at 24 hours; (d) Correlation between PMN numbers and chemiluminescence intensities at the inflamed sites induced by different types of inflammatory stimuli.

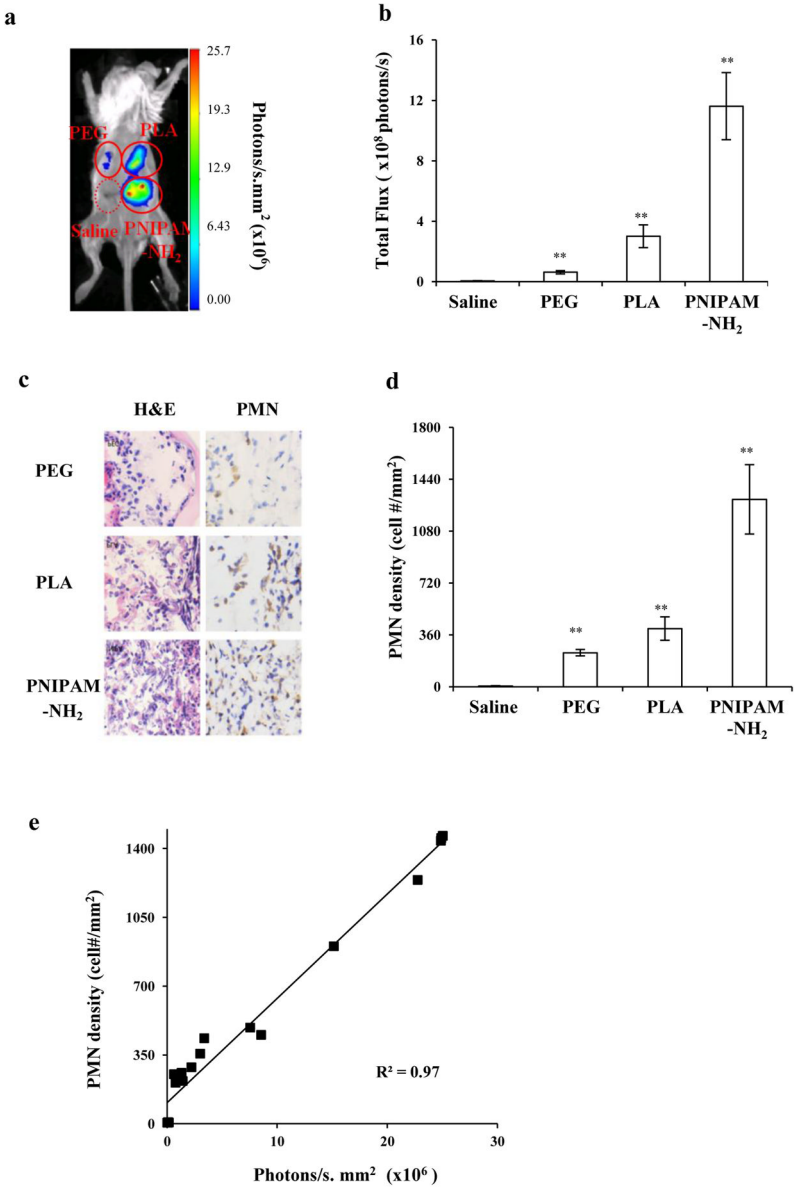

Figure 6.

(a) Chemiluminescence imaging of mice implanted subcutaneously with particles made of PNIPAM-NH_2, PLA and PEG for 24 hours; (b) Mean chemiluminescence intensities in tissue at the implantation sites; (c) Images of H&E and neutrophil staining of corresponding tissues; (d) PMNs density in tissue surrounding various particle implants; (e) Correlation between PMN numbers and chemiluminescence intensities in different implant sites.